BABAR-CONF-06/025
SLAC-PUB-11979
July 2006

Search for the Rare Decay $B^{\pm} \to a_0^{\pm}\pi^0$

The *BABAR* Collaboration

February 7, 2008

Abstract

A search for the decay $B\pm \to a_0^{\pm}\pi^0$ with the a_0^+ decaying to an η and a π^+ was carried out at the Stanford Linear Accelerator Center using the *BABAR* detector coupled with the PEP-II collider. The analysis used a data sample comprised of approximately 252 million $B\overline{B}$ pairs collected at the Υ(4S) resonance. No signal was observed and a 90% confidence level upper limit on the branching fraction was set at 1.32×10^{-6}.

Submitted to the 33rd International Conference on High-Energy Physics, ICHEP 06, 26 July—2 August 2006, Moscow, Russia.

Stanford Linear Accelerator Center, Stanford University, Stanford, CA 94309

Work supported in part by Department of Energy contract DE-AC03-76SF00515.

The *BABAR* Collaboration,

B. Aubert, R. Barate, M. Bona, D. Boutigny, F. Couderc, Y. Karyotakis, J. P. Lees, V. Poireau, V. Tisserand, A. Zghiche

Laboratoire de Physique des Particules, IN2P3/CNRS et Université de Savoie, F-74941 Annecy-Le-Vieux, France

E. Grauges

Universitat de Barcelona, Facultat de Fisica, Departament ECM, E-08028 Barcelona, Spain

A. Palano

Università di Bari, Dipartimento di Fisica and INFN, I-70126 Bari, Italy

J. C. Chen, N. D. Qi, G. Rong, P. Wang, Y. S. Zhu

Institute of High Energy Physics, Beijing 100039, China

G. Eigen, I. Ofte, B. Stugu

University of Bergen, Institute of Physics, N-5007 Bergen, Norway

G. S. Abrams, M. Battaglia, D. N. Brown, J. Button-Shafer, R. N. Cahn, E. Charles, M. S. Gill, Y. Groysman, R. G. Jacobsen, J. A. Kadyk, L. T. Kerth, Yu. G. Kolomensky, G. Kukartsev, G. Lynch, L. M. Mir, T. J. Orimoto, M. Pripstein, N. A. Roe, M. T. Ronan, W. A. Wenzel

Lawrence Berkeley National Laboratory and University of California, Berkeley, California 94720, USA

P. del Amo Sanchez, M. Barrett, K. E. Ford, A. J. Hart, T. J. Harrison, C. M. Hawkes, S. E. Morgan, A. T. Watson

University of Birmingham, Birmingham, B15 2TT, United Kingdom

T. Held, H. Koch, B. Lewandowski, M. Pelizaeus, K. Peters, T. Schroeder, M. Steinke

Ruhr Universität Bochum, Institut für Experimentalphysik 1, D-44780 Bochum, Germany

J. T. Boyd, J. P. Burke, W. N. Cottingham, D. Walker

University of Bristol, Bristol BS8 1TL, United Kingdom

D. J. Asgeirsson, T. Cuhadar-Donszelmann, B. G. Fulsom, C. Hearty, N. S. Knecht, T. S. Mattison, J. A. McKenna

University of British Columbia, Vancouver, British Columbia, Canada V6T 1Z1

A. Khan, P. Kyberd, M. Saleem, D. J. Sherwood, L. Teodorescu

Brunel University, Uxbridge, Middlesex UB8 3PH, United Kingdom

V. E. Blinov, A. D. Bukin, V. P. Druzhinin, V. B. Golubev, A. P. Onuchin, S. I. Serednyakov, Yu. I. Skovpen, E. P. Solodov, K. Yu Todyshev

Budker Institute of Nuclear Physics, Novosibirsk 630090, Russia

D. S. Best, M. Bondioli, M. Bruinsma, M. Chao, S. Curry, I. Eschrich, D. Kirkby, A. J. Lankford, P. Lund, M. Mandelkern, R. K. Mommsen, W. Roethel, D. P. Stoker

University of California at Irvine, Irvine, California 92697, USA

S. Abachi, C. Buchanan

University of California at Los Angeles, Los Angeles, California 90024, USA

S. D. Foulkes, J. W. Gary, O. Long, B. C. Shen, K. Wang, L. Zhang
University of California at Riverside, Riverside, California 92521, USA

H. K. Hadavand, E. J. Hill, H. P. Paar, S. Rahatlou, V. Sharma
University of California at San Diego, La Jolla, California 92093, USA

J. W. Berryhill, C. Campagnari, A. Cunha, B. Dahmes, T. M. Hong, D. Kovalskyi, J. D. Richman
University of California at Santa Barbara, Santa Barbara, California 93106, USA

T. W. Beck, A. M. Eisner, C. J. Flacco, C. A. Heusch, J. Kroseberg, W. S. Lockman, G. Nesom, T. Schalk, B. A. Schumm, A. Seiden, P. Spradlin, D. C. Williams, M. G. Wilson
University of California at Santa Cruz, Institute for Particle Physics, Santa Cruz, California 95064, USA

J. Albert, E. Chen, A. Dvoretskii, F. Fang, D. G. Hitlin, I. Narsky, T. Piatenko, F. C. Porter, A. Ryd, A. Samuel
California Institute of Technology, Pasadena, California 91125, USA

G. Mancinelli, B. T. Meadows, K. Mishra, M. D. Sokoloff
University of Cincinnati, Cincinnati, Ohio 45221, USA

F. Blanc, P. C. Bloom, S. Chen, W. T. Ford, J. F. Hirschauer, A. Kreisel, M. Nagel, U. Nauenberg, A. Olivas, W. O. Ruddick, J. G. Smith, K. A. Ulmer, S. R. Wagner, J. Zhang
University of Colorado, Boulder, Colorado 80309, USA

A. Chen, E. A. Eckhart, A. Soffer, W. H. Toki, R. J. Wilson, F. Winklmeier, Q. Zeng
Colorado State University, Fort Collins, Colorado 80523, USA

D. D. Altenburg, E. Feltresi, A. Hauke, H. Jasper, J. Merkel, A. Petzold, B. Spaan
Universität Dortmund, Institut für Physik, D-44221 Dortmund, Germany

T. Brandt, V. Klose, H. M. Lacker, W. F. Mader, R. Nogowski, J. Schubert, K. R. Schubert, R. Schwierz, J. E. Sundermann, A. Volk
Technische Universität Dresden, Institut für Kern- und Teilchenphysik, D-01062 Dresden, Germany

D. Bernard, G. R. Bonneaud, E. Latour, Ch. Thiebaux, M. Verderi
Laboratoire Leprince-Ringuet, CNRS/IN2P3, Ecole Polytechnique, F-91128 Palaiseau, France

P. J. Clark, W. Gradl, F. Muheim, S. Playfer, A. I. Robertson, Y. Xie
University of Edinburgh, Edinburgh EH9 3JZ, United Kingdom

M. Andreotti, D. Bettoni, C. Bozzi, R. Calabrese, G. Cibinetto, E. Luppi, M. Negrini, A. Petrella, L. Piemontese, E. Prencipe
Università di Ferrara, Dipartimento di Fisica and INFN, I-44100 Ferrara, Italy

F. Anulli, R. Baldini-Ferroli, A. Calcaterra, R. de Sangro, G. Finocchiaro, S. Pacetti, P. Patteri, I. M. Peruzzi,[1] M. Piccolo, M. Rama, A. Zallo
Laboratori Nazionali di Frascati dell'INFN, I-00044 Frascati, Italy

[1]Also with Università di Perugia, Dipartimento di Fisica, Perugia, Italy

A. Buzzo, R. Capra, R. Contri, M. Lo Vetere, M. M. Macri, M. R. Monge, S. Passaggio, C. Patrignani, E. Robutti, A. Santroni, S. Tosi

Università di Genova, Dipartimento di Fisica and INFN, I-16146 Genova, Italy

G. Brandenburg, K. S. Chaisanguanthum, M. Morii, J. Wu

Harvard University, Cambridge, Massachusetts 02138, USA

R. S. Dubitzky, J. Marks, S. Schenk, U. Uwer

Universität Heidelberg, Physikalisches Institut, Philosophenweg 12, D-69120 Heidelberg, Germany

D. J. Bard, W. Bhimji, D. A. Bowerman, P. D. Dauncey, U. Egede, R. L. Flack, J. A. Nash, M. B. Nikolich, W. Panduro Vazquez

Imperial College London, London, SW7 2AZ, United Kingdom

P. K. Behera, X. Chai, M. J. Charles, U. Mallik, N. T. Meyer, V. Ziegler

University of Iowa, Iowa City, Iowa 52242, USA

J. Cochran, H. B. Crawley, L. Dong, V. Eyges, W. T. Meyer, S. Prell, E. I. Rosenberg, A. E. Rubin

Iowa State University, Ames, Iowa 50011-3160, USA

A. V. Gritsan

Johns Hopkins University, Baltimore, Maryland 21218, USA

A. G. Denig, M. Fritsch, G. Schott

Universität Karlsruhe, Institut für Experimentelle Kernphysik, D-76021 Karlsruhe, Germany

N. Arnaud, M. Davier, G. Grosdidier, A. Höcker, F. Le Diberder, V. Lepeltier, A. M. Lutz, A. Oyanguren, S. Pruvot, S. Rodier, P. Roudeau, M. H. Schune, A. Stocchi, W. F. Wang, G. Wormser

Laboratoire de l'Accélérateur Linéaire, IN2P3/CNRS et Université Paris-Sud 11, Centre Scientifique d'Orsay, B.P. 34, F-91898 ORSAY Cedex, France

C. H. Cheng, D. J. Lange, D. M. Wright

Lawrence Livermore National Laboratory, Livermore, California 94550, USA

C. A. Chavez, I. J. Forster, J. R. Fry, E. Gabathuler, R. Gamet, K. A. George, D. E. Hutchcroft, D. J. Payne, K. C. Schofield, C. Touramanis

University of Liverpool, Liverpool L69 7ZE, United Kingdom

A. J. Bevan, F. Di Lodovico, W. Menges, R. Sacco

Queen Mary, University of London, E1 4NS, United Kingdom

G. Cowan, H. U. Flaecher, D. A. Hopkins, P. S. Jackson, T. R. McMahon, S. Ricciardi, F. Salvatore, A. C. Wren

University of London, Royal Holloway and Bedford New College, Egham, Surrey TW20 0EX, United Kingdom

D. N. Brown, C. L. Davis

University of Louisville, Louisville, Kentucky 40292, USA

J. Allison, N. R. Barlow, R. J. Barlow, Y. M. Chia, C. L. Edgar, G. D. Lafferty, M. T. Naisbit, J. C. Williams, J. I. Yi

University of Manchester, Manchester M13 9PL, United Kingdom

C. Chen, W. D. Hulsbergen, A. Jawahery, C. K. Lae, D. A. Roberts, G. Simi

University of Maryland, College Park, Maryland 20742, USA

G. Blaylock, C. Dallapiccola, S. S. Hertzbach, X. Li, T. B. Moore, S. Saremi, H. Staengle

University of Massachusetts, Amherst, Massachusetts 01003, USA

R. Cowan, G. Sciolla, S. J. Sekula, M. Spitznagel, F. Taylor, R. K. Yamamoto

Massachusetts Institute of Technology, Laboratory for Nuclear Science, Cambridge, Massachusetts 02139, USA

H. Kim, S. E. Mclachlin, P. M. Patel, S. H. Robertson

McGill University, Montréal, Québec, Canada H3A 2T8

A. Lazzaro, V. Lombardo, F. Palombo

Università di Milano, Dipartimento di Fisica and INFN, I-20133 Milano, Italy

J. M. Bauer, L. Cremaldi, V. Eschenburg, R. Godang, R. Kroeger, D. A. Sanders, D. J. Summers, H. W. Zhao

University of Mississippi, University, Mississippi 38677, USA

S. Brunet, D. Côté, M. Simard, P. Taras, F. B. Viaud

Université de Montréal, Physique des Particules, Montréal, Québec, Canada H3C 3J7

H. Nicholson

Mount Holyoke College, South Hadley, Massachusetts 01075, USA

N. Cavallo,[2] G. De Nardo, F. Fabozzi,[3] C. Gatto, L. Lista, D. Monorchio, P. Paolucci, D. Piccolo, C. Sciacca

Università di Napoli Federico II, Dipartimento di Scienze Fisiche and INFN, I-80126, Napoli, Italy

M. A. Baak, G. Raven, H. L. Snoek

NIKHEF, National Institute for Nuclear Physics and High Energy Physics, NL-1009 DB Amsterdam, The Netherlands

C. P. Jessop, J. M. LoSecco

University of Notre Dame, Notre Dame, Indiana 46556, USA

T. Allmendinger, G. Benelli, L. A. Corwin, K. K. Gan, K. Honscheid, D. Hufnagel, P. D. Jackson, H. Kagan, R. Kass, A. M. Rahimi, J. J. Regensburger, R. Ter-Antonyan, Q. K. Wong

Ohio State University, Columbus, Ohio 43210, USA

N. L. Blount, J. Brau, R. Frey, O. Igonkina, J. A. Kolb, M. Lu, R. Rahmat, N. B. Sinev, D. Strom, J. Strube, E. Torrence

University of Oregon, Eugene, Oregon 97403, USA

[2]Also with Università della Basilicata, Potenza, Italy
[3]Also with Università della Basilicata, Potenza, Italy

A. Gaz, M. Margoni, M. Morandin, A. Pompili, M. Posocco, M. Rotondo, F. Simonetto, R. Stroili, C. Voci

Università di Padova, Dipartimento di Fisica and INFN, I-35131 Padova, Italy

M. Benayoun, H. Briand, J. Chauveau, P. David, L. Del Buono, Ch. de la Vaissière, O. Hamon, B. L. Hartfiel, M. J. J. John, Ph. Leruste, J. Malclès, J. Ocariz, L. Roos, G. Therin

Laboratoire de Physique Nucléaire et de Hautes Energies, IN2P3/CNRS, Université Pierre et Marie Curie-Paris6, Université Denis Diderot-Paris7, F-75252 Paris, France

L. Gladney, J. Panetta

University of Pennsylvania, Philadelphia, Pennsylvania 19104, USA

M. Biasini, R. Covarelli

Università di Perugia, Dipartimento di Fisica and INFN, I-06100 Perugia, Italy

C. Angelini, G. Batignani, S. Bettarini, F. Bucci, G. Calderini, M. Carpinelli, R. Cenci, F. Forti, M. A. Giorgi, A. Lusiani, G. Marchiori, M. A. Mazur, M. Morganti, N. Neri, E. Paoloni, G. Rizzo, J. J. Walsh

Università di Pisa, Dipartimento di Fisica, Scuola Normale Superiore and INFN, I-56127 Pisa, Italy

M. Haire, D. Judd, D. E. Wagoner

Prairie View A&M University, Prairie View, Texas 77446, USA

J. Biesiada, N. Danielson, P. Elmer, Y. P. Lau, C. Lu, J. Olsen, A. J. S. Smith, A. V. Telnov

Princeton University, Princeton, New Jersey 08544, USA

F. Bellini, G. Cavoto, A. D'Orazio, D. del Re, E. Di Marco, R. Faccini, F. Ferrarotto, F. Ferroni, M. Gaspero, L. Li Gioi, M. A. Mazzoni, S. Morganti, G. Piredda, F. Polci, F. Safai Tehrani, C. Voena

Università di Roma La Sapienza, Dipartimento di Fisica and INFN, I-00185 Roma, Italy

M. Ebert, H. Schröder, R. Waldi

Universität Rostock, D-18051 Rostock, Germany

T. Adye, N. De Groot, B. Franek, E. O. Olaiya, F. F. Wilson

Rutherford Appleton Laboratory, Chilton, Didcot, Oxon, OX11 0QX, United Kingdom

R. Aleksan, S. Emery, A. Gaidot, S. F. Ganzhur, G. Hamel de Monchenault, W. Kozanecki, M. Legendre, G. Vasseur, Ch. Yèche, M. Zito

DSM/Dapnia, CEA/Saclay, F-91191 Gif-sur-Yvette, France

X. R. Chen, H. Liu, W. Park, M. V. Purohit, J. R. Wilson

University of South Carolina, Columbia, South Carolina 29208, USA

M. T. Allen, D. Aston, R. Bartoldus, P. Bechtle, N. Berger, R. Claus, J. P. Coleman, M. R. Convery, M. Cristinziani, J. C. Dingfelder, J. Dorfan, G. P. Dubois-Felsmann, D. Dujmic, W. Dunwoodie, R. C. Field, T. Glanzman, S. J. Gowdy, M. T. Graham, P. Grenier,[4] V. Halyo, C. Hast, T. Hryn'ova, W. R. Innes, M. H. Kelsey, P. Kim, D. W. G. S. Leith, S. Li, S. Luitz, V. Luth, H. L. Lynch, D. B. MacFarlane, H. Marsiske, R. Messner, D. R. Muller, C. P. O'Grady, V. E. Ozcan, A. Perazzo, M. Perl, T. Pulliam, B. N. Ratcliff, A. Roodman, A. A. Salnikov, R. H. Schindler, J. Schwiening, A. Snyder, J. Stelzer, D. Su, M. K. Sullivan, K. Suzuki, S. K. Swain, J. M. Thompson, J. Va'vra, N. van

[4]Also at Laboratoire de Physique Corpusculaire, Clermont-Ferrand, France

Bakel, M. Weaver, A. J. R. Weinstein, W. J. Wisniewski, M. Wittgen, D. H. Wright, A. K. Yarritu, K. Yi, C. C. Young

Stanford Linear Accelerator Center, Stanford, California 94309, USA

P. R. Burchat, A. J. Edwards, S. A. Majewski, B. A. Petersen, C. Roat, L. Wilden

Stanford University, Stanford, California 94305-4060, USA

S. Ahmed, M. S. Alam, R. Bula, J. A. Ernst, V. Jain, B. Pan, M. A. Saeed, F. R. Wappler, S. B. Zain

State University of New York, Albany, New York 12222, USA

W. Bugg, M. Krishnamurthy, S. M. Spanier

University of Tennessee, Knoxville, Tennessee 37996, USA

R. Eckmann, J. L. Ritchie, A. Satpathy, C. J. Schilling, R. F. Schwitters

University of Texas at Austin, Austin, Texas 78712, USA

J. M. Izen, X. C. Lou, S. Ye

University of Texas at Dallas, Richardson, Texas 75083, USA

F. Bianchi, F. Gallo, D. Gamba

Università di Torino, Dipartimento di Fisica Sperimentale and INFN, I-10125 Torino, Italy

M. Bomben, L. Bosisio, C. Cartaro, F. Cossutti, G. Della Ricca, S. Dittongo, L. Lanceri, L. Vitale

Università di Trieste, Dipartimento di Fisica and INFN, I-34127 Trieste, Italy

V. Azzolini, N. Lopez-March, F. Martinez-Vidal

IFIC, Universitat de Valencia-CSIC, E-46071 Valencia, Spain

Sw. Banerjee, B. Bhuyan, C. M. Brown, D. Fortin, K. Hamano, R. Kowalewski, I. M. Nugent, J. M. Roney, R. J. Sobie

University of Victoria, Victoria, British Columbia, Canada V8W 3P6

J. J. Back, P. F. Harrison, T. E. Latham, G. B. Mohanty, M. Pappagallo

Department of Physics, University of Warwick, Coventry CV4 7AL, United Kingdom

H. R. Band, X. Chen, B. Cheng, S. Dasu, M. Datta, K. T. Flood, J. J. Hollar, P. E. Kutter, B. Mellado, A. Mihalyi, Y. Pan, M. Pierini, R. Prepost, S. L. Wu, Z. Yu

University of Wisconsin, Madison, Wisconsin 53706, USA

H. Neal

Yale University, New Haven, Connecticut 06511, USA

1 INTRODUCTION

The quark content of the a_0 mesons is a subject of debate. It has been conjectured that they may not be simple $q\overline{q}$ states but may have a more complex nature [1] such as having a $K\overline{K}$ component, being a glueball, or being a mixture of two and four quark states. According to Delepine *et al.* [2], a measurement of the branching fraction (BF) of $B^+ \to a_0^+\pi^0$ may help in resolving this problem, as the predicted branching fraction for the four quark model is expected to be up to an order of magnitude less than the two quark model. The predicted branching fraction for this is already small, of order 2×10^{-7}.

Assuming the two quark model, the proposed Feynman diagrams for the dominant tree level decays are given in Fig. 1. The low expected branching fraction is explained by the fact that the colour suppressed diagram (b) is expected to dominate over the colour allowed diagram (a) since the colour allowed case is also doubly suppressed by G-parity and vector current conservation [3]. Due to this it is also not possible to use isospin arguments to relate the branching fraction for this mode to others in the same final state Dalitz plane, such as $B^+ \to a_0^0\pi^+$.

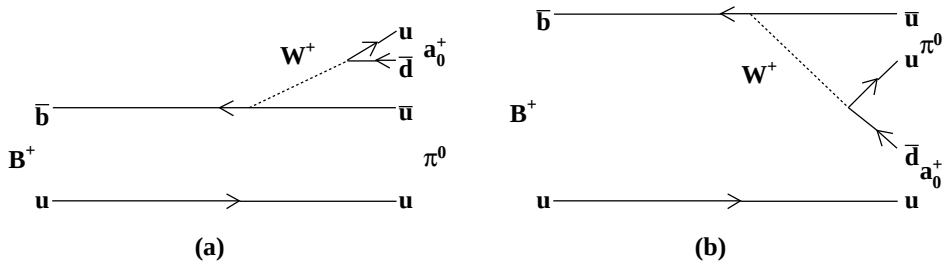

Figure 1: The proposed Feynman diagrams for the process $B^+ \to a_0^+\pi^0$ with (a) external (color allowed) production of the a_0^+ and (b) internal (color suppressed) production of the a_0^+.

The aim of the analysis described in this paper is to better constrain the existing models by measuring the BF for the decay $B^+ \to a_0^+\pi^0$. The analysis focuses solely on the case where the a_0^+ decays to an η and a π^+, with the η decaying to two photons. This sub-mode accounts for $\approx 40\%$ of all η decays. An unbinned extended maximum likelihood fit (ML) method is used to extract the $B^+ \to a_0^+\pi^0$ event yield. Throughout this document the conjugate decay mode $B^- \to a_0^-\pi^0$ is implied and a_0 refers to the $a_0(980)$ unless stated otherwise.

2 THE *BABAR* DETECTOR & DATASET

The analysis was performed using data collected with the *BABAR* detector [4] at the PEP-II asymmetric-energy e^+e^- collider [5] at the Stanford Linear Accelerator Center. Charged particles are detected and their momenta measured with a 5-layer double sided silicon vertex tracker (SVT) and a 40-layer drift chamber (DCH) inside a 1.5 T solenoidal magnet. A quartz bar ring-

imaging Čerenkov detector (DIRC) complements the $\mathrm{d}E/\mathrm{d}x$ measurement in the DCH for the identification of charged particles. Energies of neutral particles are measured by an electromagnetic calorimeter (EMC) composed of 6,580 CsI(Tl) crystals, and the instrumented magnetic flux return (IFR) is used to identify muons.

The data sample consists of $229.8\,\mathrm{fb}^{-1}$ collected at the $\Upsilon(4\mathrm{S})$ resonance. The number of $B\overline{B}$ pairs used in the analysis totals $(252.2 \pm 2.8) \times 10^6$ [6].

3 RECONSTRUCTION & SELECTION

The analysis was based on the reconstruction of final states consisting of four photons and one π^+. All charged particle tracks were taken as π^+ candidates unless they were identified as kaons by a particle identification algorithm based on DCH and DIRC information. Tracks were required to have momentum $\leq 10\,\mathrm{GeV}/c$ with transverse momentum $\geq 0.1\,\mathrm{GeV}/c$. They were also required to be composed from ≥ 12 DCH hits and with a distance of closest approach to the interaction region within 1.5 cm in the transverse direction and 10 cm along the axis of the detector.

In order to construct η candidates, all pairs of photons in each event were combined. The individual photons were required to have energy between 0.05 and 10 GeV. The invariant mass of each candidate pair was then required to be between 0.515 and $0.569\,\mathrm{GeV}/c^2$. This required mass range was optimised by maximising the ratio of signal to the square root of the background, $S/\sqrt{B}$, using signal and background Geant4 Monte Carlo (MC) samples.

The η candidates were refitted to constrain their mass to the known value [7] and were then combined with the π^+ candidates to form a_0^+ candidates, which were required to have a mass between 0.8 and $1.2\,\mathrm{GeV}/c^2$. The a_0^+ mass selection was left relatively loose as this variable was used in the ML fit.

Pairs of photons in the event were also used to form π^0 candidates. The photons were required to have energy between 0.03 and 10 GeV. The π^0 candidates were required to be consistent with the mass of a π^0, i.e. in the range 0.115 to $0.150\,\mathrm{GeV}/c^2$. The π^0 candidates were also refitted to constrain their mass to the known value [7].

B meson candidates were formed by combining all a_0^+ and π^0 candidates in the event. The B candidates were described kinematically using the energy substituted mass $m_{\mathrm{ES}} = [(\frac{1}{2}s + \vec{p}_0.\vec{p}_B)^2/E_0^2 - |\vec{p}_B|^2]^{\frac{1}{2}}$ and the energy difference $\Delta E = E_B^* - \frac{1}{2}\sqrt{s}$. Here, $\vec{p}_B$ and E_B are the momentum and energy of the B candidate, $\vec{p}_0$ and E_0 are the momentum and energy of the initial (e^+, e^-) state and the * indicates this quantity is expressed in the centre-of-mass system. $\sqrt{s}$ is the CM energy. Both m_{ES} and ΔE were included in the ML fit with the requirements, $5.20 < m_{\mathrm{ES}} < 5.29\,\mathrm{GeV}/c^2$ and $|\Delta E| < 0.35\,\mathrm{GeV}$. Since event reconstruction is an imperfect process more then one candidate was produced for each B. The average number of B candidates per signal event was observed in signal MC to be 1.38. Further selection based on the quality of these candidates was not performed and all were included in the ML fit sample. The fit was designed, as explained and verified in section 5, to only pick up one candidate per event.

4 BACKGROUNDS

The major background in this analysis comes from random combinations of particles in continuum $e^+e^- \to q\overline{q}$ events ($q = u,d,s,c$). These were primarily rejected by placing a requirement on the cosine of the angle between the thrust axis of the reconstructed B candidate and the thrust axis of

Table 1: The charmless modes identified as potentially contributing significantly to the background. The nominal contributions used in the fit are given.

Decay Mode	Expected Yield (B candidates)
Charm B decays	
Charged $b \to c$	322 ± 32
Neutral $b \to c$	200 ± 20
Charmless B decays	
$B^{\pm} \to \rho^{\pm}\pi^0$	78 ± 10
$B^{\pm} \to a_1^{\pm}\pi^0$	58 ± 13
$B^{\pm} \to \rho^{\pm}\eta$	37^{+8}_{-7}
$B^{\pm} \to \rho^{\pm}(1450)\eta$	25 ± 25
$B^0 \to \pi^0\pi^0$	19 ± 4
Inclusive $B \to X_s\gamma$	18^{+5}_{-4}
$B^0 \to \eta\pi^0$	14 ± 14
$B^0 \to a_0^{\pm}\rho^{\mp}$	12 ± 12
$B^{\pm} \to a_0^0\rho^{\pm}$	6 ± 6
$B^{\pm} \to a_0^{\pm}(1450)\pi^0$	5 ± 5
$B^{\pm} \to \pi^{\pm}\eta\pi^0$ (non-resonant)	2 ± 2
$B^{\pm} \to \pi^{\pm}\pi^0\pi^0$ (non-resonant)	2 ± 2

the rest of the event, $|\cos(\theta_{TB})|$; the thrust was calculated in the CM frame. The distribution of this variable peaks sharply near 1.0 for the two jet-like combinations from continuum $q\overline{q}$ pairs and is approximately uniform for B meson pairs; $|\cos(\theta_{TB})|$ was required to satisfy $|\cos(\theta_{TB})| < 0.594$. This requirement was chosen by again maximising $S/\sqrt{B}$ using signal and background MC samples.

In order to further separate signal from continuum a Fisher discriminant $\mathcal{F}$ [8] was used in the ML fit. The discriminant was a weighted linear combination of the absolute value of the cosine of the angle between the direction of the B candidate momentum and the beam axis, $|\cos(\theta_{TB})|$ as defined above, and the L_0 and L_2 Legendre polynomial projections of the energy flow of the event with respect to the B candidate thrust axis. The L_0 and L_2 quantities were formed by summing over all the neutral and charged particles in the event which were not used to form the B candidate. The Fisher discriminant was required to satisfy $-3 < \mathcal{F} < 1$.

The $B\overline{B}$ background was split into charmed and charmless decay components, both of which were accounted for in the fit. The charmed component was modelled by removing the charmless component from the $B\overline{B}$ MC sample. The charmless contributions were selected by studying B decays in MC with identical or similar final states to the signal decay. Further contributions were identified from general charmless B decay MC samples which pass the selection criteria. These modes were modelled using exclusive MC samples. From the final state Dalitz plot we expect only 1 significant peaking background ($B^{\pm} \to \rho^{\pm}(1450)\eta$) to overlap our signal. The other modes which contribute are mainly present through some degree of mis-reconstruction. All B background yields were held fixed at their expected values in the final fit. The expected contributions for these modes are listed in Table 1.

5 MAXIMUM LIKELIHOOD FIT

The input variables to the extended ML fit were $m_{\rm ES}$, ΔE, $\mathcal{F}$, and the a_0^+ resonance mass. The probability density functions (PDF) used to model the data are discussed below, and were determined from MC simulation. The exception to this is the continuum component where most parameters were left free in the fit, thus enabling us to extract the parameters directly from the data. The only other floated quantities in the fit were the signal and continuum yields.

5.1 Signal Model

The peaking components in ΔE and $m_{\rm ES}$ were modelled with a Novosibirsk function [9] and two independent Gaussians respectively. The $\mathcal{F}$ shape was modelled using an asymmetric Gaussian and the a_0^+ resonance mass with a Breit-Wigner. The resonance was modelled in signal MC with a mass of $0.98\,{\rm GeV}/c^2$ and a width of $80\,{\rm MeV}/c^2$ [10].

The signal shape can be distorted by true signal candidates which have been mis-reconstructed and is referred to as self-crossfeed (SXF). The B candidates affected have more background-like distributions in the fit variables. If improperly accounted for these can result in a reduction of the discriminating power of the fit.

In some signal events one true B candidate was seen as well as a number of SXF B candidates. As stated in Section 3 this gives an average of 1.38 B candidates per event. In order to remove any distortion which may result from SXF, therefore giving the purest possible signal shape, a model was created which combines the expected true signal shape (described above) with a model to describe the SXF. High purity samples of signal and SXF were used for this purpose. The true signal sample was obtained from MC by requiring that all generated daughter particles of the signal decay were correctly reconstructed. This method was not 100% efficient, leading to cross-contamination between the signal and SXF samples. In order to minimise this effect the signal and SXF samples were fitted iteratively to determine the PDF parameters. The SXF model was not explicitly included in the final fit since its purpose was to facilitate the removal of SXF distortion from the signal shape. The resulting PDFs, projected onto signal MC, are presented in figure 2.

It was verified that there was negligible contamination of the signal component with SXF events and that these were instead absorbed by the continuum PDF. It was also verified that this method yields no greater than one good signal candidate per event, despite the inclusion of multiple candidates. The tests are outlined in Section 5.3.

5.2 Background Model

Any peaking contributions in $m_{\rm ES}$ and ΔE in the background samples were modelled using Gaussian shapes. Where a slowly varying, combinatorial component exists it was modelled with low-order polynomials in ΔE and an ARGUS [11] threshold function for $m_{\rm ES}$. In most charmless modes correlations were expected to exist between these variables. In order to model these correlations the above prescription was, where necessary, replaced with a two-dimensional non-parametric KEYS PDF [12]. $\mathcal{F}$ was modelled either with two Gaussians or an asymmetric Gaussian. Peaking components in the a_0^+ mass variable were modelled with Gaussians or Breit-Wigners depending on mis-reconstruction. Any more slowly varying components were modelled with low-order polynomials.

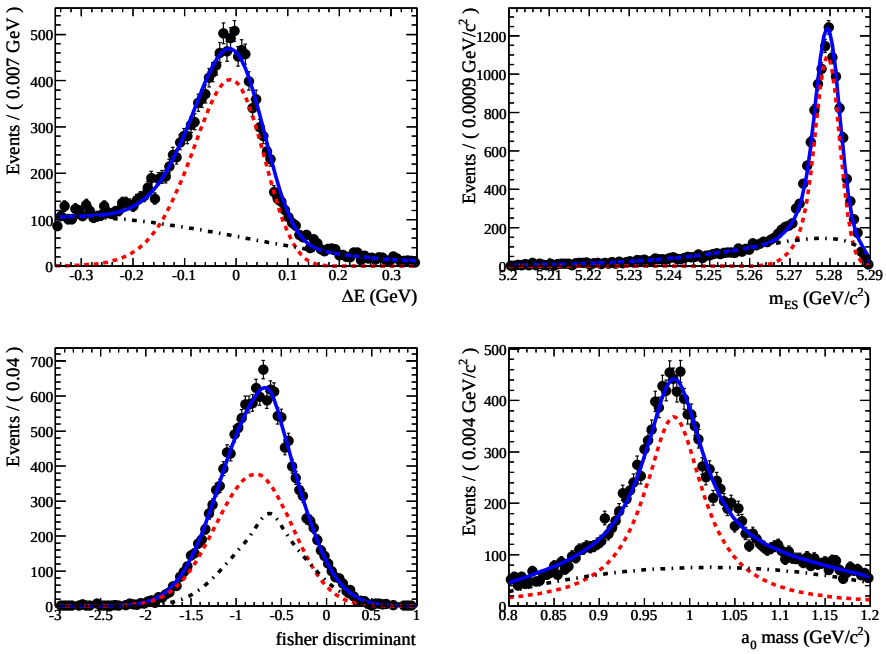

Figure 2: Signal model PDFs projected onto signal MC. The total PDF is given in blue (solid line) with the true signal contribution in red (dashed) and the SXF in black (dash-dotted). Only the true signal shape is used in the final fit.

5.3 Fit Validation

In order to verify the consistency of the fitting procedure MC simulations were generated from the PDF model. By refitting to these datasets and assessing the shifts in the fitted signal yields any problems with the model could be detected. In the studies no significant deviation from the generated signal yield was found. In order to detect biases from any improperly modelled correlations among the variables the above study was repeated with embedded randomly selected events from the fully simulated signal and background MC samples. No significant biases from any of the background modes were found, nor from any correlations in signal MC. Any small biases which exist were used to estimate a systematic error contribution. Finally, in order to test the ability of the fit to separate true signal from SXF, SXF candidates were explicitly embedded from the signal MC and a check for shifts in the fitted signal yield was made. Once again the fitted signal yields were consistent with those expected.

6 SYSTEMATIC STUDIES

The systematic uncertainties fall into three categories: firstly the errors in the number of events extracted from the fit, secondly the errors in the efficiency, and lastly the errors in the BF result due to uncertainties in the total number of B mesons and in the daughter BFs.

6.1 Systematic errors derived from the fit

Uncertainties resulting from the ML fit give additive systematic errors in the number of signal events derived from the fit.

- Uncertainties in the PDF parameters used in the fit
  This uncertainty lies in the statistical errors in the fitted parameters of the PDFs which make up the model. These were due to the limited amount of available MC simulated events upon which to model any given PDF. Each parameter in a PDF was considered independent of the others, thus neglecting any correlations which may exist. The PDFs considered were signal, $B\overline{B}$ events with charmless modes removed, and continuum. The charmless contribution was expected to be small and was neglected. With the exception of the signal a_0 mass Breit-Wigner width, all of the parameters were varied within their errors and the final fit repeated. In all cases the resulting shifts in the fitted signal yield were taken as the systematic error contribution. For the signal a_0 mass Breit-Wigner width lower and upper bounds of $50\,\mathrm{MeV}/c^2$ and $100\,\mathrm{MeV}/c^2$ were assumed. This was to account for the uncertainty in the modelled a_0 lineshape.

- Uncertainties in charmless B decay contributions
  The uncertainty here lies in the normalisation of the separate charmless backgrounds due to errors in the BFs used to estimate their contribution. These values are listed in Table 1. The systematic error contribution was calculated as the shift in the fitted signal yield in the final fit to data where the contributions from each specific mode were varied within the errors of their BFs. For the cases where only an upper limit exists, the contributions were calculated assuming 50% of the limit as a central value. The systematic error was then estimated by varying this assumed central value by $\pm 100\%$.

- Uncertainties in the yields of the $B \to$ charm modes
  This uncertainty was ascertained by varying the yields of the B to charmed modes by $\pm 10\%$ as a conservative estimate. This yield uncertainty was dominated by the error in the efficiency for reconstructing these B modes and not the cross-section for their production. Once again the shifts in the signal yield were taken as systematic errors.

- Uncertainties in the bias from the fit
  To estimate any potential fit bias, a simulation study was run embedding all B backgrounds from the MC and generating continuum MC according to the values of the continuum shape parameters resulting from the final fit. Zero signal events were embedded or generated. The systematic error was estimated as the sum in quadrature of 50% of the fitted bias and its statistical error.

6.2 Systematic errors in the efficiency

There are a number of sources of systematic uncertainty which affect the efficiency and are thus applied as a multiplicative correction to the final result.

- Tracking and neutrals efficiencies
  This source of uncertainty arises in tracking where a global per track systematic error of 0.5% was assigned based on results of dedicated studies. There was also an uncertainty in the efficiency for reconstructing neutral particles. A systematic error of 3% each for every π^0 and η in the final state was assigned.

- Data/MC agreement in the $|\cos\theta_{TB}|$ variable
  Due to the imperfect agreement between data and MC samples, the selection criteria for $|\cos\theta_{TB}|$ require the assignment of a systematic error. Control sample studies have shown that tighter selections incur larger errors. As such a conservative 5% error due to this selection was assigned.

- Statistical error
  Finally, the error due to limited MC statistics in the efficiency had to be accounted for. This was simply the binomial error in selecting a given number of events from a larger sample.

6.3 Systematic errors contributing to the branching fraction

These systematic contributions are also multiplicative errors.

- Total number of $B\overline{B}$ events
  The total number of $B\overline{B}$ events in the data set was estimated to be $(252.2 \pm 2.8) \times 10^6$. The error was taken as a systematic.

- Uncertainties in the daughter decay BFs
  The errors in $\mathcal{B}(a_0^+ \to \eta\pi^+)$ and $\mathcal{B}(\eta \to \gamma\gamma)$ were taken from the Particle Data Group [7]. The error in $\mathcal{B}(a_0^+ \to \eta\pi^+)$ was calculated by taking the ratio of the partial widths of the two dominant a_0^+ decay modes; $a_0^+ \to \eta\pi^+$ and $a_0^+ \to K\overline{K}$. The measured ratio is 0.183 ± 0.024 which, assuming all other decay modes are negligible, gives $\mathcal{B}(a_0^+ \to \eta\pi^+) = 0.85 \pm 0.02$. The value taken for $\mathcal{B}(\eta \to \gamma\gamma)$ was 0.3943 ± 0.0026.

6.4 Summary of Systematics

The results of all of the studies to estimate systematic error are presented in Table 2.

Table 2: Estimated systematic errors in the final fit result.

Source of Uncertainty	$\eta \to \gamma\gamma$
Additive (Events)	
Fit Parameters	$^{+7.7}_{-4.4}$
Charmless Yields	$^{+2.3}_{-1.5}$
Charm Yields	$^{+0.2}_{-0.0}$
Fit Bias	± 1.6
Total Additive (Events)	$^{+8.2}_{-4.9}$
Multiplicative (%)	
Neutral efficiency	± 6.0
Tracking efficiency	± 0.5
$\|\cos(\theta_{TB})\|$ Selection	± 5.0
MC Statistics	± 0.9
Number of $B\overline{B}$ Events	± 1.1
Daughter a_0 Decay BF	± 2.0
Daughter η Decay BF	± 0.7
Total Multiplicative (%)	± 8.2

7 RESULTS

The results from the fit to the full data set are given in Table 3. The yield is found to be consistent with zero.

Table 3: The results of the fit to the full data set and other values required for calculating the branching fraction. All B background yields were held fixed to the values listed in Table 1. The upper limit is shown first with only the statistical error and then with the total error.

Required quantity/result	
Candidates to fit	36098
Signal Yield (events)	-18±11
Continuum Yield (candidates)	35324±190
ML Fit bias (events)	2.55
Accepted eff. and BFs	
ϵ (%)	16.18
$\mathcal{B}(\eta \to \gamma\gamma)$ (%)	39.43
$\mathcal{B}(a_0^+ \to \eta\pi^+)$ (%)	84.5
Results	
Branching Fraction ($\times 10^{-6}$)	$-1.5^{+0.9}_{-0.7}(stat)^{+0.6}_{-0.4}(syst)$
Upper Limit 90% C.L. ($\times 10^{-6}$)	< 1.06 (statistical error only)
Upper Limit 90% C.L. ($\times 10^{-6}$)	< 1.32 (total error)

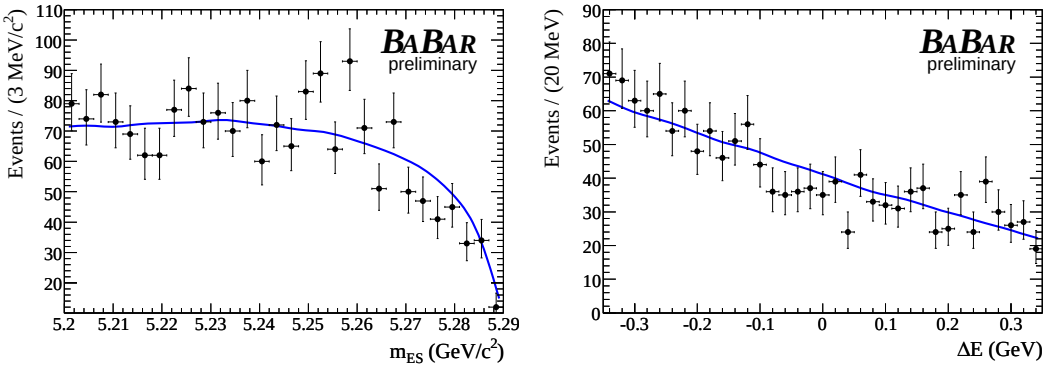

Figure 3: Projection plots in $m_{\rm ES}$ and ΔE comparing MC generated from the overall PDF (blue solid curve) with the data (black points). The samples have been background reduced by requiring the ratio of likelihoods $\mathcal{L}_{sig}/[\mathcal{L}_{sig} + \Sigma\mathcal{L}_{bkg}]$ to be > 0.6.

The branching fraction is calculated using the following formula

$$\mathcal{B} = \frac{Y - Y_B}{\epsilon N_{B\overline{B}} \Pi_i \mathcal{B}_i} \tag{1}$$

where Y is the signal event yield from the fit, Y_B is the fit bias, ϵ is the efficiency for the B decaying via the studied mode, $N_{B\overline{B}}$ is the number of produced $B\overline{B}$ mesons and $\Pi_i\mathcal{B}_i$ is the product of the

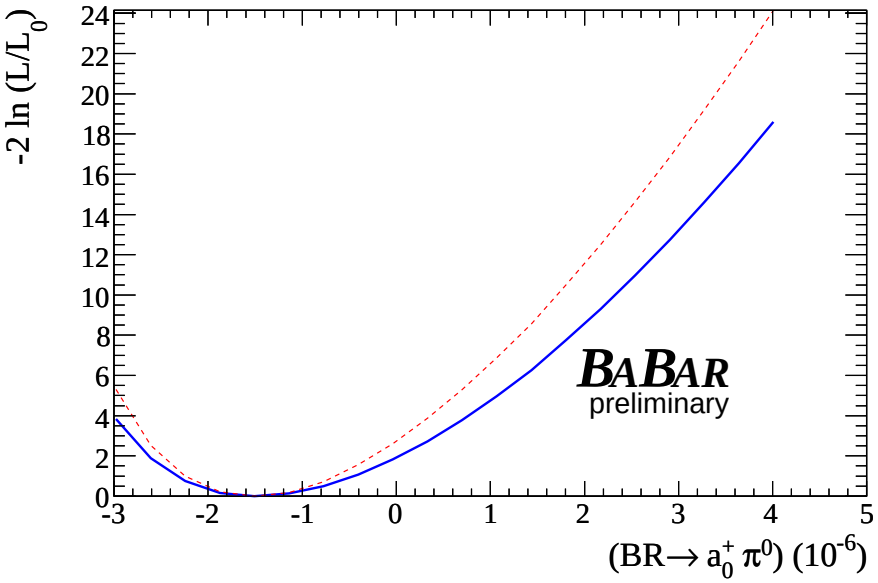

Figure 4: Log likelihood scan curve showing the effect of convoluting in systematic errors. The red dashed curve shows the likelihood for statistical errors only while the blue solid curve shows the likelihood including systematic errors.

daughter branching fractions. The decay rates for $\Upsilon(4S) \to B^+B^-$ and $\Upsilon(4S) \to B^0\overline{B}^0$ are assumed to be equal.

Projection plots for the final fit results are presented in Figure 3. These compare a sample of MC generated from the overall PDF with the data. Both samples have had background reduced by requiring that the likelihood ratio $\mathcal{L}_{sig}/[\mathcal{L}_{sig} + \Sigma\mathcal{L}_{bkg}]$ for any event be > 0.6.

The likelihood $\mathcal{L}$ was convoluted with a Gaussian to include the systematic errors. A scan was performed to give the variation in the likelihood for different input yields. The resulting curve in $-2\ln(\mathcal{L}/\mathcal{L}_0)$ as a function of the branching fraction is shown in Fig. 4. Note how this plot is scaled relative to the value for the minimum negative log likelihood ($\mathcal{L}_0$). From this distribution the upper limit of 1.32×10^{-6} was computed by integrating the associated likelihood function to find the yield which bounds 90% of the area under the curve. In doing this a starting branching fraction value of zero was assumed.

This upper limit is reported in Table 3 with and without the systematic error to indicate the degree to which the limit is statistics dominated. The largest source of systematic error comes from the a_0 lineshape.

8 SUMMARY

A search for the decay $B^+ \to a_0^+\pi^0$ was carried out using 252 million $B\overline{B}$ pairs. An unbinned extended maximum likelihood fit was used to obtain the result. The fitted signal yield was consistent with zero and thus a 90% C.L. upper limit of 1.32×10^{-6} was set on the branching fraction for this decay. Our sensitivity to this mode was therefore insufficient to make it possible to differentiate between the two and four quark a_0 structure models as defined by Delepine *et al.* [2].

9 ACKNOWLEDGMENTS

The authors are grateful for the extraordinary contributions of our PEP-II colleagues in achieving the excellent luminosity and machine conditions that have made this work possible. The success of this project also relies critically on the expertise and dedication of the computing organizations that support *BABAR*. The collaborating institutions wish to thank SLAC for its support and the kind hospitality extended to them. This work is supported by the US Department of Energy and National Science Foundation, the Natural Sciences and Engineering Research Council (Canada), Institute of High Energy Physics (China), the Commissariat à l'Energie Atomique and Institut National de Physique Nucléaire et de Physique des Particules (France), the Bundesministerium für Bildung und Forschung and Deutsche Forschungsgemeinschaft (Germany), the Istituto Nazionale di Fisica Nucleare (Italy), the Foundation for Fundamental Research on Matter (The Netherlands), the Research Council of Norway, the Ministry of Science and Technology of the Russian Federation, and the Particle Physics and Astronomy Research Council (United Kingdom). Individuals have received support from the Marie-Curie IEF program (European Union) and the A. P. Sloan Foundation.

References

[1] V. Baru *et al.*, Phys. Lett. **B586**, 53 (2004).

[2] D. Delepine *et al.*, Eur. Phys. J. C**45**, 693 (2006).

[3] S. Laplace *et al.*, Eur. Phys. J. C**22**, 431 (2001).

[4] The *BABAR* Collaboration, B. Aubert *et al.*, Nucl. Instrum. Methods **A479**, 1 (2002).

[5] PEP-II Conceptual Design Report, SLAC-R-418 (1993).

[6] The *BABAR* Collaboration, B. Aubert *et al.*, Phys. Rev. **D67**, 032002 (2003).

[7] Particle Data Group, S. Eidelman *et al.*, Phys. Lett. **B592**, 1 (2004).

[8] R. A. Fisher, Annals of Eugenics **7**, 179 (1936).

[9] The Novosibirsk function is defined as $f(x) = A_s \exp(-0.5(\ln^2[1 + \Lambda\tau(x - x_0)]/\tau^2 + \tau))$ where $\Lambda = \sinh(\tau\sqrt{\ln 4})/(\sigma\tau\sqrt{\ln 4})$, the peak is x_0 and τ is the tail parameter.

6

[10] The *BABAR* Collaboration, B. Aubert *et al.*, Phys. Rev. **D70**, 111102 (2004).

[11] The ARGUS function is defined as $f(x) = x[(1 - (x/E_{beam}))^2 \exp[p(1 - (x/E_{beam}))^2]]^{1/2}$.

[12] K. S. Cranmer, Comput. Phys. Commun. **136**, 198 (2001).